

# A Boron-Containing PAH as a Substructure of Boron-Doped Graphene\*\*

Chuangdong Dou, Shohei Saito,\* Kyohei Matsuo, Ichiro Hisaki, and Shigehiro Yamaguchi\*

Graphene, a two-dimensional (2D) honeycomb lattice of  $sp^2$ -hybridized carbon atoms, is a most attractive material because of its extraordinary thermal, mechanical, and electrical properties. It holds enormous potential for widespread applications, such as nanoscale electronic devices, composite materials, sensors, solar cells, hydrogen storage, and electrodes for Li-ion batteries.<sup>[1]</sup> However, its application to nanoscale transistors is impeded by its intrinsic zero-band-gap character.<sup>[2]</sup> Intensive studies have recently been conducted to address this issue by opening and tuning the band gap, which endows the graphene with semiconducting properties. One approach is the synthesis of graphene nanoribbons with defined widths and edges, which enables its chemical and electronic properties to be tuned.<sup>[3]</sup> The other promising strategy is chemical doping with B or N atoms.<sup>[4]</sup> In particular, B-doped graphene has currently attracted increasing attention as a high-performance field-effect transistor (FET) material as well as an anode material for high-power Li-ion batteries.<sup>[4a,b]</sup>

Despite the intensive theoretical and experimental studies on the chemistry of B-doped graphene, the synthesis of well-defined B-doped graphenes remains a challenge. The preparation methods reported to date, such as chemical vapor deposition, solution-phase reductive coupling, and thermal annealing, only produce a mixture of B-doped graphenes with various molecular weights, edge shapes, and doping positions.<sup>[5]</sup> In this context, the bottom-up organic synthesis should have a significant advantage in producing a fragment of B-doped graphene as a single compound and enable the precise elucidation of its molecular properties, as is the case of

undoped nanographene flakes.<sup>[6]</sup> However, the synthesis of “B-doped nanographene”<sup>[7]</sup> has been hampered by the intrinsic instability of tricoordinated organoboranes to oxygen and moisture. To overcome this issue, N atoms are often concomitantly introduced into polycyclic skeletons in the form of B-N units.<sup>[8]</sup> The interaction between the lone pair of electrons on the N atom and the empty p orbital of the B atom enhances the stability, but, at the same time, degrades the inherent characteristics of the B atom, such as Lewis acidity and electron-accepting properties. We recently proposed a “structural constraint” as an alternative strategy for the stabilization. We synthesized a planar triphenylborane constrained with methylene tethers and demonstrated its remarkable stability to oxygen and water, despite the absence of steric protection on the B atom.<sup>[9]</sup> However, the  $\pi$  conjugation is not fully expanded over the entire molecule because of the  $sp^3$  carbon tethers. A breakthrough to compensate for this shortcoming was made when a triarylborane was produced in which three aryl groups are directly fused with one another.<sup>[10]</sup> The highly planar and conjugated skeleton indeed enabled it to form the face-to-face  $\pi$  stacking in the crystalline state and demonstrate intriguing photophysical properties, although its structure is still far from the nanographene type. Herein, we disclose the first bottom-up organic synthesis of a B-doped nanographene, which consists of all  $sp^2$ -hybridized carbon hexagons with a well-defined B-embedded structure in terms of the number of B atoms incorporated as well as their positions. The impact of the boron doping on the electronic structure of the extended polycyclic aromatic hydrocarbon (PAH) has been precisely elucidated.

We have now designed a B-containing PAH **1** as a substructure of B-doped graphene. Its parent honeycomb lattice **2** composed of 15 hexagons should be intriguing due to its singlet biradical character similar to teranthene (see the Supporting Information).<sup>[11]</sup> Since the replacement of a C atom by a B atom corresponds to a one-electron oxidation, namely hole doping,<sup>[12]</sup> the doping of a single B atom into the skeleton will result in the formation of an unstable open-shell compound (Scheme 1). Two boron atoms need to be introduced at the same time to produce a stable closed-shell structure. In compound **1**, two B atoms are placed in the central hexagon, and its closed-shell structure should produce unique properties that are totally different from those of the undoped congener **2**.

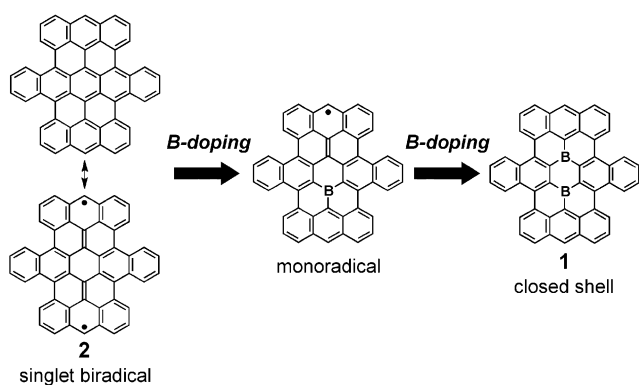
Compound **1a** was synthesized by the oxidative cyclo-dehydrogenation (intramolecular Scholl reaction) of a 6,13-dihydro-6,13-diborapentacene precursor **3** bearing an orthogonal anthryl group on each boron atom (Scheme 2). Bulky mesityloxy substituents are introduced at the 4,5-positions of

[\*] Dr. C. Dou, Dr. S. Saito, K. Matsuo, Prof. Dr. S. Yamaguchi  
Department of Chemistry  
Graduate School of Science  
Nagoya University, and  
CREST (Japan) Science and Technology Agency  
Furo, Chikusa, Nagoya 464-8602 (Japan)  
E-mail: s\_saito@chem.nagoya-u.ac.jp  
yamaguchi@chem.nagoya-u.ac.jp

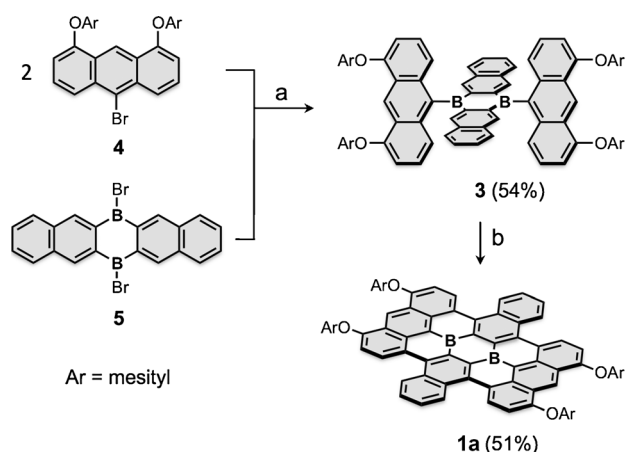
Dr. I. Hisaki  
Department of Material and Life Science, Graduate School of  
Engineering, Osaka University (Japan)

[\*\*] This work was supported by CREST and JST (S.Y.), by a Grant-in-Aid for Young Scientists (B) (24750038, to S.S.), and a Grant-in-Aid for Young Scientists (A) (24685026, to I.H.). Crystallographic data collection was performed at the BL38B1 in the SPring-8 at the BL38B1 with approval of JASRI (proposal No. 2012A1809). We thank Prof. T. Kubo, A. Konishi (Osaka University), Prof. H. Shinokubo, and Dr. S. Hiroto (Nagoya University) for their approval to use their spectral data. PAH = polycyclic aromatic hydrocarbon.

Supporting information for this article is available on the WWW under <http://dx.doi.org/10.1002/anie.201206699>.



**Scheme 1.** Stepwise boron doping of an extended polyaromatic hydrocarbon.



**Scheme 2.** Synthesis of B-doped nanographene **1a**. Reagents and conditions: a) **4**, *n*BuLi, Et<sub>2</sub>O, from 0 °C to 25 °C, then **5**, toluene, from 0 °C to 25 °C; b) FeCl<sub>3</sub>, CH<sub>3</sub>NO<sub>2</sub> and CH<sub>2</sub>Cl<sub>2</sub>.

the anthracene moieties for the cyclization to occur selectively at the 1,8-positions and to prevent the strong aggregation of the resulting PAH  $\pi$  skeleton. This anthryl group was originally reported by Anderson and coworkers, and is widely used for the synthesis of expanded  $\pi$  skeletons.<sup>[13]</sup>

The precursor **3** was prepared in 54% yield by the lithiation of 9-bromobis(mesityloxy)anthracene **4**<sup>[13]</sup> with *n*BuLi, followed by treatment with dibromodiborapentacene **5**.<sup>[14]</sup> Compound **3** showed high stability to water and oxygen as a result of the steric protection of the boron atoms by the bulky anthryl groups. The cyclodehydrogenation of **3** with an excess of FeCl<sub>3</sub> proceeded successfully to form **1a** in 51% yield as a deep purple solid. As expected, the doubly B-doped nanographene **1a** is stable enough to handle in air and was isolated by column chromatography on silica gel without any special precautions. Compound **1a** is sufficiently soluble in common organic solvents, such as chlorobenzene (4.8 mg mL<sup>-1</sup>) and *ortho*-dichlorobenzene (10.8 mg mL<sup>-1</sup>), thus demonstrating its processability in solution.

The structure of **1** was unambiguously characterized by mass spectrometry, NMR spectroscopy (Figure 1), and finally X-ray crystallography (Figure 2). These analyses revealed **1a** to be a single compound. High-resolution atmospheric

pressure chemical ionization time-of-flight (APCI-TOF) MS showed a parent ion signal for **1a** at *m/z* 1157.4942 (calcd for C<sub>84</sub>H<sub>63</sub>O<sub>4</sub>B<sub>2</sub> [M+H]<sup>+</sup>, *m/z* 1157.4931; see the Supporting Information). Two sets of coupled signals (H<sup>a</sup> and H<sup>b</sup>, and H<sup>c</sup> and H<sup>d</sup> in Figure 1) were observed at 6.96 and 9.12 ppm, and 7.76 and 9.02 ppm, respectively in the <sup>1</sup>H NMR spectrum

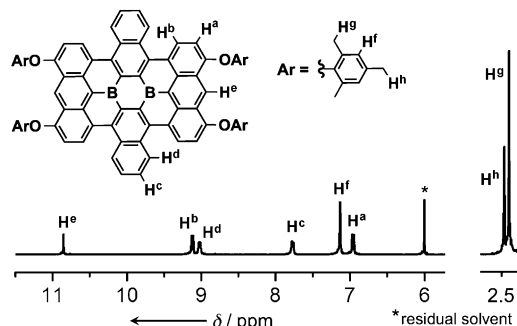


**Figure 1.** <sup>1</sup>H NMR spectrum of **1a** in [D<sub>2</sub>]tetrachloroethane at 353 K.

of **1a** in [D<sub>2</sub>]tetrachloroethane at 353 K (Figure 1). The relatively downfield chemical shifts of the H<sup>b</sup> and H<sup>d</sup> signals are attributed to the deshielding effect by the ring current of the neighboring benzene rings in the cove region. The other deshielded singlet signal at 10.85 ppm corresponds to the H<sup>e</sup> atom, which reflects the close contact with the oxygen atoms (see the Supporting Information).<sup>[13]</sup> Variable-temperature <sup>1</sup>H NMR measurements from 193 to 353 K did not show any significant change. This temperature independency indicates a large energy gap between the singlet closed-shell ground state and a triplet excited state. The gap was calculated theoretically to be 34.9 kcal mol<sup>-1</sup> for **1a** at the B3LYP/6-31G\* level, which is far larger than that of the parent undoped nanographene **2** (1.5 kcal mol<sup>-1</sup>) with an open-shell ground state (see the Supporting Information). The broad <sup>11</sup>B NMR signal of **1a** at 58.0 ppm is typical of tricoordinated boron compounds.

The single crystals were obtained by slow diffusion of heptane into a solution of **1a** in chlorobenzene. The X-ray crystallographic analysis revealed a contorted polycyclic skeleton of the B-doped nanographene **1a** composed of 48 sp<sup>2</sup>-hybridized C atoms and two tricoordinated B atoms (Figure 2).<sup>[15]</sup> Fifteen six-membered rings are fused to form the nanographene sheet with four cove regions and two zigzag edges. As a consequence of steric overcrowding of the H<sup>b</sup> and H<sup>d</sup> atoms in the cove regions, the  $\pi$ -conjugated core skeleton is distorted away from planarity. Although the distance between the most deviated C atoms and the C<sub>48</sub>B<sub>2</sub> mean plane is 1.02 Å, the dihedral angles between the most contorted benzene rings and the central C<sub>4</sub>B<sub>2</sub> ring is 19.7°. The doping positions of the two B atoms were determined unambiguously, as the B–C bond lengths of 1.507(2), 1.531(2), and 1.535(2) Å are significantly longer than those of the other C–C bonds (1.37–1.48 Å). Notably, these B–C bonds are much shorter than those of the nonfused triphenylborane (1.57–1.59 Å).<sup>[16]</sup> This structural characteristic has already been observed in the other planarized triarylboranes pre-

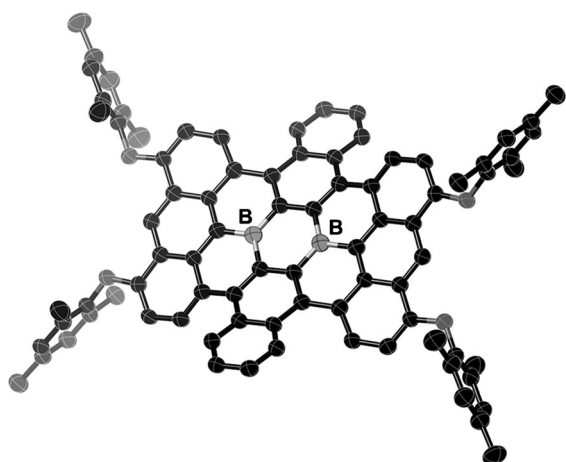


**Figure 2.** X-ray crystal structure of **1a** (50% probability for thermal ellipsoids).

viously synthesized by our research group.<sup>[9,10]</sup> The B atoms take an ideal trigonal planar geometry, with the sum of the three C-B-C angles being 360.0°.  $\pi$  stacking of the nanographene skeletons was not observed in the packing structure because of the steric hindrance of the bulky mesityl groups. The mesityl groups are almost perpendicular to the  $\pi$  framework, which suppresses the strong aggregation and guarantees the sufficient solubility in organic solvents.

The photophysical properties of **1a** help to understand the impact of replacing C atoms with B atoms in extended PAHs. A solution of **1a** in toluene has a purple color (Figure 3). The

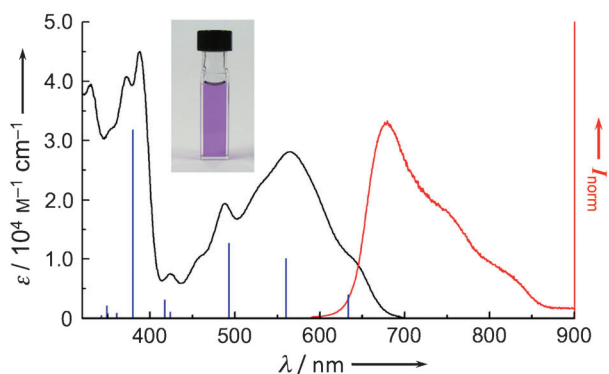


**Figure 3.** UV/Vis absorption (black line) and Vis/near-IR fluorescence (red line,  $\lambda_{\text{ex}} = 570$  nm) spectra of **1a** in toluene, along with the oscillator strengths (blue bars) obtained by TD-DFT (B3LYP/6-31G\*) calculations. Inset: photograph of **1a** in toluene.

broad absorption bands in the UV/Vis absorption spectrum recorded in toluene cover the entire visible region of 400–700 nm, with maxima ( $\lambda_{\text{abs}}$ ) at 564 and 487 nm, and with a shoulder band at 640 nm. In general, the absorption spectra of polyaromatic hydrocarbons (PAHs) depend on the size and the edge shapes.<sup>[17]</sup> The stable PAHs with armchair-type edges (so-called fully benzenoid PAHs) have relatively shorter  $\lambda_{\text{abs}}$  values for their sizes. When compared to stable benzenoid

PAHs of similar sizes, such as hexabenzocoronene (42  $\text{sp}^2$ -hybridized C atoms;  $\lambda_{\text{abs}} = 361$  and 392 nm),<sup>[18]</sup> the B-containing PAH **1a** has a significantly red-shifted  $\lambda_{\text{abs}}$  value (see the Supporting Information). On the other hand, the  $\lambda_{\text{abs}}$  value of **1a** is blue-shifted when compared to those of reactive PAHs with zigzag edges, such as extended acenes,<sup>[19]</sup> rylene,<sup>[20]</sup> and anthenes.<sup>[11,21]</sup> In particular, teranthene, which has a singlet biradical character and whose spectrum should be similar to that of the undoped congener **2**, shows absorption bands in the near-IR region ( $\lambda_{\text{abs}} = 878$  and 1054 nm),<sup>[11]</sup> but it gradually decomposes under ambient conditions (see the Supporting Information). Taking these comparisons into consideration, one may conclude that “B doping” results in the nanographenes having broad absorption bands in the long-wavelength visible region, while maintaining their stability.

The other important feature of the B-doped nanographene is its fluorescence. The emission spectrum of compound **1a** shows a broad fluorescence band in the visible/near-IR region with a maximum ( $\lambda_{\text{em}}$ ) at 679 nm, although the quantum yield is low ( $\Phi = 0.04$ ). Fluorescence reaching the near-IR region is rare in undoped nanographenes. Fluorescences comparable to that of **1a** have only been reported for supernaphthalene ( $\lambda_{\text{em}} = 611$  nm)<sup>[22]</sup> and quaterrylene ( $\lambda_{\text{em}} = 680$  nm).<sup>[23]</sup> The emission spectra of **1a** as well as its absorption spectra showed negligible solvent effects (see the Supporting Information).

DFT calculations were performed at the B3LYP/6-31G\* level of theory to more precisely elucidate the electronic structure of **1** (Figure 4). The optimized structure reproduced

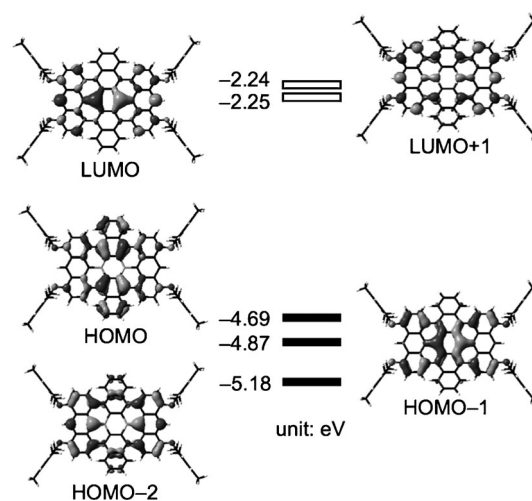


**Figure 4.** Kohn–Sham molecular orbitals of **1a**, based on calculations at the B3LYP/6-31G\* level.

well the distorted structure of the cove regions observed in the crystal structure (see the Supporting Information). The calculation showed that the orbitals of the B atoms contribute to the HOMO-1 and LUMO to a significant extent. The transition energies and oscillator strengths simulated by the TD-DFT (B3LYP/6-31G\*) calculations showed a good agreement with the observed absorption spectrum of **1a** (Figure 3 and see the Supporting Informa-

tion). The absorption bands observed at 640, 564, and 487 nm are assignable to the electronic transitions HOMO→LUMO, HOMO-1→LUMO+1, and HOMO-2→LUMO, with reasonable oscillator strengths of 0.103, 0.262 and 0.328, respectively. It is notable that all these transitions involve either the HOMO-1 or LUMO. Namely, the contribution of the p orbitals of the B atoms is responsible for the intense and broad absorption bands observed in the visible region.

Since the doubly B-doped nanographene **1a** is isoelectronic with the dicationic species of the undoped nanographene **2<sup>2+</sup>**, we compared their electronic structures theoretically (see Figure S19 in the Supporting Information). Although the energy levels are significantly different from each other, because of the positive charge of **2<sup>2+</sup>**, the molecular orbitals of these compounds are similarly distributed, except for the LUMO and HOMO-1 in **1a**. Since these orbitals have large orbital coefficients at the doping positions, the replacement of the C atoms with B atoms perturbs the energy levels of these orbitals. The replacement tends to relatively elevate their energy levels. As a result, the HOMO-1 and HOMO as well as the LUMO and LUMO+1 in **1a** are closer in energy than those in **2<sup>2+</sup>**. It is also worth noting that the molecular orbital distributions of **1a** are not perturbed by the introduction of the mesityloxy substituents, although their energy levels are elevated by 0.3–0.5 eV (see the Supporting Information).

The electrochemical properties of the B-doped nanographene are important for applications in nanoscale transistors or Li-ion battery electrodes. The sufficient solubility of **1a** enabled cyclic voltammetry measurements in THF (Figure 5). Regardless of the scan rates, reversible redox

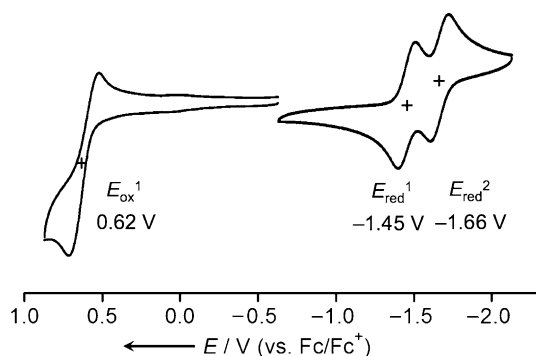


**Figure 5.** Cyclic voltammogram of **1a** in THF (1.0 mM). Scan rate: 100 mVs<sup>-1</sup>, working electrode: glassy carbon, reference electrode: Ag/AgNO<sub>3</sub>, electrolyte: nBu<sub>4</sub>NPF<sub>6</sub>. Fc/Fc<sup>+</sup> = ferrocene/ferrocenium.

waves were observed at a first oxidation potential of  $E_{\text{ox}}^1 = +0.62$  V and at first and second reduction potentials of  $E_{\text{red}}^1 = -1.45$  V and  $E_{\text{red}}^2 = -1.66$  V (versus Fc/Fc<sup>+</sup>). These redox stabilities were also confirmed in CH<sub>2</sub>Cl<sub>2</sub> (see the Supporting Information). The high stability of the second reduction process is characteristic for **1a**, and different from the previous polycyclic monoboron  $\pi$  system<sup>[10]</sup> because of the intrinsic electron deficiency of the doubly B-doped nanographene **1a**. This reducibility should be beneficial for applications in high capacity batteries.

In summary, we have achieved the bottom-up organic synthesis of a stable “B-doped nanographene” as a single closed-shell compound. In contrast to B-doped graphenes prepared by conventional methods, this compound has a well-defined structure, including the doping positions of the B atoms. The crystal structure revealed it to deviate from planarity because of steric overcrowding in the cove regions. The most important impact of the “B doping” is the significant contributions of the p orbitals of the B atoms to both the relevant unoccupied and occupied orbitals, which play important roles in the broad absorption over the entire visible region as well as the fluorescence in the near-IR region. The two B atoms are also crucial for gaining the reversible multiredox properties. This study will provide a benchmark for future structural engineering of B-doped graphenes.<sup>[4]</sup> More detailed analyses of this B-doped nanographene are currently underway, including studies of the Lewis acidity, the carrier mobility, and its performance as a Li-ion battery electrode.

Received: August 18, 2012

Published online: October 19, 2012

**Keywords:** boron · fluorescence · graphene · nanostructures · polycyclic aromatic hydrocarbons

- [1] For recent reviews and articles on graphene, see a) C. N. R. Rao, A. K. Sood, K. S. Subrahmanyam, A. Govindaraj, *Angew. Chem.* **2009**, *121*, 7890; *Angew. Chem. Int. Ed.* **2009**, *48*, 7752; b) M. J. Allen, V. C. Tung, R. B. Kaner, *Chem. Rev.* **2010**, *110*, 132; c) K. P. Loh, Q. Bao, P. K. Ang, J. Yang, *J. Mater. Chem.* **2010**, *20*, 2277; d) F. Schwierz, *Nat. Nanotechnol.* **2010**, *5*, 487; e) P. Avouris, *Nano Lett.* **2010**, *10*, 4285; f) S. Pang, Y. Hernandez, X. Feng, K. Müllen, *Adv. Mater.* **2011**, *23*, 2779; g) Z. Sun, D. K. James, J. M. Tour, *J. Phys. Chem. Lett.* **2011**, *2*, 2425.
- [2] a) K. S. Novoselov, A. K. Geim, S. V. Morozov, D. Jiang, Y. Zhang, S. V. Dubonos, I. V. Grigorieva, A. A. Firsov, *Science* **2004**, *306*, 666; b) C. Berger, Z. Song, X. Li, X. Wu, N. Brown, C. Naud, D. Mayou, T. Li, J. Hass, A. N. Marchenkov, E. H. Conrad, P. N. First, W. A. de Heer, *Science* **2006**, *312*, 1191.
- [3] a) X. Li, X. Wang, L. Zhang, S. Lee, H. Dai, *Science* **2008**, *319*, 1229; b) D. V. Kosynkin, A. L. Higginbotham, A. Sinitskii, J. R. Lomeda, A. Dimiev, B. K. Price, J. M. Tour, *Nature* **2009**, *458*, 872; c) L. Jiao, L. Zhang, X. Wang, G. Diankov, H. Dai, *Nature* **2009**, *458*, 877; d) J. Cai, P. Ruffieux, R. Jaafar, M. Bieri, T. Braun, S. Blankenburg, M. Muoth, A. P. Seitsonen, M. Saleh, X. Feng, K. Müllen, R. Fasel, *Nature* **2010**, *466*, 470.
- [4] a) Y.-B. Tang, L.-C. Yin, Y. Yang, X.-H. Bo, Y.-L. Cao, H.-E. Wang, W.-J. Zhang, I. Bello, S.-T. Lee, H.-M. Cheng, C.-S. Lee, *ACS Nano* **2012**, *6*, 1970; b) Z.-S. Wu, W. Ren, L. Xu, F. Li, H.-M. Cheng, *ACS Nano* **2011**, *5*, 5463; c) H. Wang, T. Maiyalagan, X. Wang, *ACS Catal.* **2012**, *2*, 781; d) H. Liu, Y. Liu, D. Zhu, *J. Mater. Chem.* **2011**, *21*, 3335; e) X. Wang, X. Li, L. Zhang, Y. Yoon, P. K. Weber, H. Wang, J. Guo, H. Dai, *Science* **2009**, *324*, 768.
- [5] a) T. Shirasaki, A. Derré, M. Ménétrier, A. Tressaud, S. Flandrois, *Carbon* **2000**, *38*, 1461; b) Z. Jin, Z. Sun, L. J. Simpson, K. J. O'Neill, P. A. Parilla, Y. Li, N. P. Stadie, C. C. Ahn, C. Kittrell, J. M. Tour, *J. Am. Chem. Soc.* **2010**, *132*, 15246; c) X. Lü, J. Wu, T. Lin, D. Wan, F. Huang, X. Xie, M. Jiang, *J. Mater. Chem.* **2011**, *21*, 10685; d) Z.-H. Sheng, H.-L. Gao, W.-J. Bao, F.-B. Wang, X.-H. Xia, *J. Mater. Chem.* **2012**, *22*, 390.

- [6] a) L. Chen, Y. Hernandez, X. Feng, K. Müllen, *Angew. Chem.* **2012**, *124*, 7758; *Angew. Chem. Int. Ed.* **2012**, *51*, 7640; b) J. Wu, W. Pisula, K. Müllen, *Chem. Rev.* **2007**, *107*, 718; c) K. N. Plunkett, K. Godula, C. Nuckolls, N. Tremblay, A. C. Whalley, S. Xiao, *Org. Lett.* **2009**, *11*, 2225; d) X. Yan, X. Cui, L.-S. Li, *J. Am. Chem. Soc.* **2010**, *132*, 5944; e) K. Mochida, K. Kawasumi, Y. Segawa, K. Itami, *J. Am. Chem. Soc.* **2011**, *133*, 10716.
- [7] We use the terminology “B-doped nanographene” to represent a nanometer-sized honeycomb lattice structure in which more than one B atoms are embedded.
- [8] a) T. Torres, *Angew. Chem.* **2006**, *118*, 2900; *Angew. Chem. Int. Ed.* **2006**, *45*, 2834; b) M. J. D. Bosdet, W. E. Piers, T. S. Sorensen, M. Parvez, *Angew. Chem.* **2007**, *119*, 5028; *Angew. Chem. Int. Ed.* **2007**, *46*, 4940; c) Z. Liu, T. B. Marder, *Angew. Chem.* **2008**, *120*, 248; *Angew. Chem. Int. Ed.* **2008**, *47*, 242; d) P. J. Brothers, *Chem. Commun.* **2008**, 2090; e) T. Hatakeyama, S. Hashimoto, S. Seki, M. Nakamura, *J. Am. Chem. Soc.* **2011**, *133*, 18614.
- [9] Z. G. Zhou, A. Wakamiya, T. Kushida, S. Yamaguchi, *J. Am. Chem. Soc.* **2012**, *134*, 4529.
- [10] S. Saito, K. Matsuo, S. Yamaguchi, *J. Am. Chem. Soc.* **2012**, *134*, 9130.
- [11] A. Konishi, Y. Hirao, M. Nakano, A. Shimizu, E. Botek, B. Champagne, D. Shiomi, K. Sato, T. Takui, K. Matsumoto, H. Kurata, T. Kubo, *J. Am. Chem. Soc.* **2010**, *132*, 11021. The spin contamination  $\langle S^2 \rangle$  of the corresponding undoped graphene was calculated to be 1.08.
- [12] S.-S. Yu, W.-T. Zheng, *Nanoscale* **2010**, *2*, 1069.
- [13] a) N. K. S. Davis, A. L. Thompson, H. L. Anderson, *Org. Lett.* **2010**, *12*, 2124; b) N. K. S. Davis, A. L. Thompson, H. L. Anderson, *J. Am. Chem. Soc.* **2011**, *133*, 30; c) L. Zeng, C. Jiao, X. Huang, K.-W. Huang, W.-S. Chin, J. Wu, *Org. Lett.* **2011**, *13*, 6026; d) K. Naoda, H. Mori, N. Aratani, B. S. Lee, D. Kim, A. Osuka, *Angew. Chem.* **2012**, *124*, 9994; *Angew. Chem. Int. Ed.* **2012**, *51*, 9856.
- [14] J. Chen, J. W. Kampf, A. J. Ashe III, *Organometallics* **2008**, *27*, 3639.
- [15] CCDC 895660 (**1a**) contains the supplementary crystallographic data for this paper. These data can be obtained free of charge from The Cambridge Crystallographic Data Centre via [www.ccdc.cam.ac.uk/data\\_request/cif](http://www.ccdc.cam.ac.uk/data_request/cif).
- [16] F. Zettler, H. D. Hausen, H. Hess, *J. Organomet. Chem.* **1974**, *72*, 157.
- [17] R. Rieger, K. Müllen, *J. Phys. Org. Chem.* **2010**, *23*, 315.
- [18] M. Kastler, J. Schmidt, W. Pisula, D. Sebastiani, K. Müllen, *J. Am. Chem. Soc.* **2006**, *128*, 9526.
- [19] B. Purushothaman, M. Bruzek, S. R. Parkin, A.-F. Miller, J. E. Anthony, *Angew. Chem.* **2011**, *123*, 7151; *Angew. Chem. Int. Ed.* **2011**, *50*, 7013.
- [20] K.-H. Koch, K. Müllen, *Chem. Ber.* **1991**, *124*, 2091.
- [21] J. Li, K. Zhang, X. Zhang, K.-W. Huang, C. Chi, J. Wu, *J. Org. Chem.* **2010**, *75*, 856.
- [22] D. Wasserfallen, M. Kastler, W. Pisula, W. A. Hofer, Y. Fogel, Z. Wang, K. Müllen, *J. Am. Chem. Soc.* **2006**, *128*, 1334.
- [23] S. A. Tucker, H. Darmodjo, W. E. Acree, J. C. Fetzer, M. Zander, *Appl. Spectrosc.* **1992**, *46*, 1260.